PROGRESS IN PHOTOVOLTAICS: RESEARCH AND APPLICATIONS
Prog. Photovolt: Res. Appl. 2005; **13**:325–331
Published online 11 May 2005 in Wiley InterScience (www.interscience.wiley.com). DOI: 10.1002/pip.594

Research

Effect of Dissociation of Iron–Boron Pairs in Crystalline Silicon on Solar Cell Properties

Jan Schmidt*,†
Institut für Solarenergieforschung Hameln/Emmerthal (ISFH), Am Ohrberg 1, D-31860 Emmerthal, Germany

The effect of dissociation of interstitial iron-substitutional boron (Fe_iB_s) pairs, as it occurs under illumination in iron-contaminated silicon solar cells, on the solar cell properties has been studied on the basis of numerical device simulations using reported recombination parameters for Fe_i and Fe_iB_s. Most cell parameters are found to degrade during Fe_iB_s dissociation. However, the open-circuit voltage can also increase within certain ranges of the iron concentration. Critical iron concentrations are determined, giving the threshold contamination level above which a significant degradation in the corresponding cell parameter can be observed. The threshold iron contamination level of the open-circuit voltage degradation is found to be up to two orders of magnitude larger than the threshold iron level of the short-circuit current degradation. As the behaviour of the cell parameters under illumination is specific to the dissociation of Fe_iB_s pairs, the characteristic changes in the cell parameters due to illumination may be used as a simple way of identifying iron contamination problems in silicon solar cells. Copyright © 2005 John Wiley & Sons, Ltd.

KEY WORDS: silicon; solar cells; defects; recombination

INTRODUCTION

Interstitial iron (Fe_i) is a major contaminant in solar-grade crystalline silicon materials. As its energy level is close to the middle of the silicon bandgap and the electron capture cross-section is relatively large, it acts as a highly effective recombination centre in *p*-type silicon, reducing the carrier lifetime severely. In particular in solar-grade multicrystalline silicon materials, surprisingly high iron contamination levels above $\sim 10^{14}\,\mathrm{cm}^{-3}$ have been measured recently by neutron activation analysis (NAA).[1,2] Comparing these NAA results with lifetime measurements, it becomes obvious that only a small fraction of the total iron content in these materials is present in the form of interstitial iron, and the residual iron exists in a less recombination active state, presumably in the form of precipitates.[2] Using calibrated lifetime measurements, typical interstitial iron concentrations in block-cast multicrystalline silicon of $\sim 10^{12}\,\mathrm{cm}^{-3}$ have been detected in as-grown material, and Fe_i concentrations in the range of $(1\text{–}4) \times 10^{11}\,\mathrm{cm}^{-3}$ have been measured after phosphorus gettering

* Correspondence to: Dr Jan Schmidt, Institut für Solarenergieforschung Hameln/Emmerthal (ISFH), Am Ohrberg 1, D-31860 Emmerthal, Germany.
†E-mail: j.schmidt@isfh.de

Contract/grant sponsors: State of Lower Saxony; German Federal Ministry for the Environment, Nature Conservation and Nuclear Safety (BMU); contract/grant number: 0329846E.

Received 27 August 2004
Revised 2 October 2004

inherent in standard cell processing.[3,4] Owing to the heat treatment during phosphorus gettering, iron precipitates are believed to dissolve into interstitial iron atoms, reducing the effectiveness of the gettering treatment and resulting in non-negligible Fe_i concentrations even after an optimised phosphorus-gettering treatment.

In boron-doped *p*-type silicon, Fe_i is well known[5] to form pairs with substitutional boron (B_s). These Fe_iB_s pairs dissociate into Fe_i and B_s under illumination owing to an electronically stimulated defect reaction (recombination-enhanced dissociation).[6] If the silicon sample is kept in the dark at room temperature, the Fe_iB_s pairs re-form within a couple of hours. Owing to this characteristic behaviour, the carrier lifetime in iron-contaminated boron-doped silicon is determined either by Fe_iB_s pairs, isolated Fe_i or a combination of both species, depending on the pre-treatment of the sample. As both recombination centres show very different recombination properties in silicon, the injection level dependence of the corresponding carrier lifetimes is much more pronounced for isolated Fe_i than for Fe_iB_s pairs, and both injection-dependent lifetime curves show a characteristic crossover point at an approximately fixed excess carrier concentration. In this paper, the effect of the pronounced change in the lifetime caused by the dissociation of iron–boron pairs on the solar cell properties is studied on the basis of numerical device simulations using reported recombination parameters for Fe_i and Fe_iB_s.

RECOMBINATION ACTIVITY OF Fe_iB_s AND Fe_i

Table I shows the energy levels and capture cross-sections reported for isolated Fe_i and Fe_iB_s pairs in crystalline silicon.[5,7] On the basis of these data, injection-level-dependent carrier lifetimes in *p*-type silicon were calculated for various doping concentrations N_{dop} using the Shockley-Read-Hall (SRH) equation.[8,9] As can be seen from Figure 1, the Fe_iB_s pair produces a very weak injection dependence, whereas the isolated Fe_i results in a very pronounced dependence of the lifetime on the excess carrier concentration. The very different recombination properties of Fe_i and Fe_iB_s are mainly due to the fact that the ratio of electron to hole capture cross-section σ_n/σ_p is much larger for Fe_i than for Fe_iB_s. Moreover, the energetic position of Fe_iB_s is relatively shallow, making the lifetime under low-injection conditions doping-dependent, whereas Fe_i acts as a deep centre. One important consequence of the very different electronic defect parameters of Fe_i and Fe_iB_s is the existence of a crossover point of the corresponding injection-dependent lifetime curves in *p*-type silicon. For doping concentrations relevant to solar cell applications this crossover point occurs at an approximately fixed value (see Figure 1), as was recently noted by Macdonald *et al.*[4] The position of the crossover point can be easily calculated for the case of complete dissociation of Fe_iB_s into Fe_i and B_s, equating the SRH lifetimes of both recombination centres. Solving this equation for the crossover point Δn_{cr} and taking into account that the hole capture cross-section of Fe_i is a few orders of magnitude smaller than all other capture cross-sections involved, results in the simple expression

$$\Delta n_{cr} = \frac{\left(\sigma_{n,FeB}^{-1} - \sigma_{n,Fe}^{-1}\right)}{\sigma_{p,Fe}^{-1}} N_{dop} + \frac{\sigma_{p,Fe}}{\sigma_{p,FeB}} N_C \exp\left(\frac{E_{t,FeB} - E_C}{kT}\right) \quad (1)$$

where $N_C = 2{\cdot}86 \times 10^{19}\,cm^{-3}$ is the effective density of states in the conduction band. Obviously, the crossover point depends linearly on the doping concentration. However, if N_{dop} is sufficiently small the first term in Equation (1) can be neglected and the second summand determines Δn_{cr}. Using the recombination parameters

Table I. Energy levels and capture cross-sections for Fe_i and the acceptor state of the Fe_iB_s pair

Recombination centre	Energy level (eV)	σ_n (cm^2)	σ_p (cm^2)	σ_n/σ_p
Fe_i	$E_V + 0{\cdot}38$	5×10^{-14}	7×10^{-17}	714
Fe_iB_s (acceptor state)	$E_C - 0{\cdot}23$	3×10^{-14}	2×10^{-15}	15

The donor state of the Fe_iB_s pair has not to be taken into account as it is a very shallow centre ($E_t = E_V + 0{\cdot}1$ eV) showing only negligible recombination activity. Data taken from the literature[5,7].

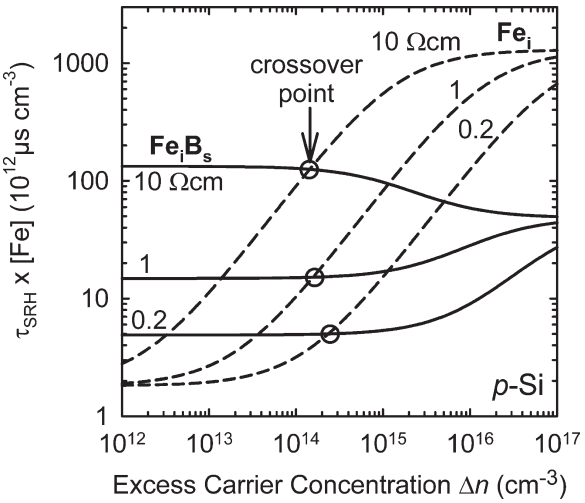

Figure 1. Calculated Shockley-Read-Hall lifetime τ_{SRH} times the iron concentration [Fe] as a function of excess carrier concentration Δn for Fe_iB_s ($[Fe_iB_s] = [Fe]$, solid lines) and Fe_i ($[Fe_i] = [Fe]$, dashed lines) in 0·2, 1 and 10 Ω cm *p*-type silicon

listed in Table I, the doping concentration dependence of the crossover point can be neglected for doping concentrations $N_{dop} \ll 1{\cdot}5 \times 10^{17}\,cm^{-3}$ and the crossover point is fixed at $\Delta n_{cr} = 1{\cdot}4 \times 10^{14}\,cm^{-3}$ at 300 K. Note that the same result is obtained for the more realistic case of an incomplete dissociation.[4]

Experimental values[4] of the crossover point reported in the literature for *p*-type silicon samples with resistivities between 0·7 and 50 Ω cm range from 1 to $3{\cdot}6 \times 10^{14}\,cm^{-3}$. Regarding the fact that these data has been measured by completely different measurement techniques, the agreement with the calculated crossover point is quite reasonable. This may also be regarded as an indirect confirmation of the recombination parameters given in Table I.

SOLAR CELL SIMULATIONS

Changes in the solar cell parameters due to the dissociation of iron–boron pairs within the base of the cell have been studied for different iron concentrations $[Fe] \equiv [Fe_i] + [Fe_iB_s]$ and various base doping concentrations N_{dop} using the device simulation tool PC1D V5·8 (P.A. Basore and D. A. Clugsten, University of New South Wales, Sydney, Australia, 2002). Two different crystalline silicon solar cell structures have been considered, both of them having a cell thickness of 300 µm (the effect of the cell thickness will be briefly discussed below). The first device structure represents a typical industrial silicon solar cell with an n^+-emitter sheet resistance of 40 Ω/□, a p^+ back surface field (BSF) at the rear and no surface passivation. The thickness of the BSF was set at 8 µm and the minority-carrier diffusion length in the BSF at 1 µm. No surface texture, but an optimal antireflection coating and a front metal grid shading of 10% were assumed. In addition, a series resistance of $1\,\Omega\,cm^2$ was implemented. The second device corresponds to a high-efficiency solar cell with a single front diffusion, a passivated front and rear surface and local contacts at the rear (no BSF). Surface recombination velocities of $S_{front} = 10000$ cm/s and $S_{rear} = 100$ cm/s have been assumed at the front and rear surface, respectively. The sheet resistance of the n^+-emitter was set at 100 Ω/□ and the front surface was pyramid-textured and antireflection-coated. In all simulations, the electronic parameters for Fe_iB_s and Fe_i shown in Table I have been used.

Figure 2 shows the changes in the short-circuit current density J_{sc}, the open-circuit voltage V_{oc}, the fill factor FF and the efficiency η of an industrial 3·5 Ω cm silicon solar cell for Fe concentrations varying between 10^9 and $10^{14}\,cm^{-3}$. The solid line was calculated using the Fe_iB_s recombination parameters and assuming that all interstitial iron is bound to boron, i.e., $[Fe_iB_s] = [Fe]$. For the sake of simplicity, complete dissociation of the Fe_iB_s

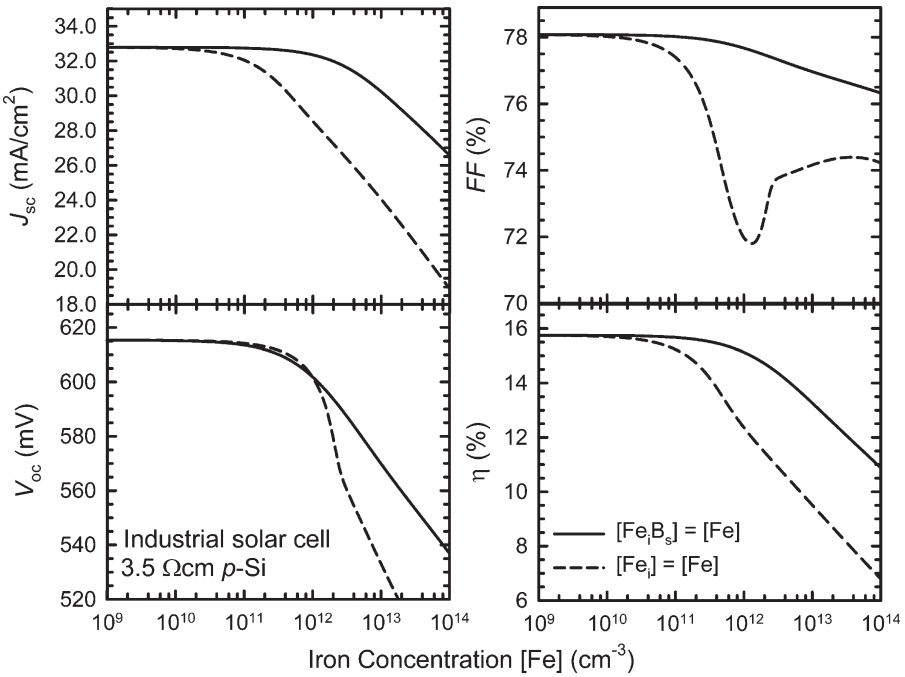

Figure 2. Short-circuit current density J_{sc}, open-circuit voltage V_{oc}, fill factor FF and efficiency η as a function of iron concentration [Fe] for a 3·5 Ω cm industrial solar cell before and after complete dissociation of Fe_iB_s pairs

pairs was assumed. Hence, after dissociation the recombination parameters of Fe_i were used and $[Fe_i] = [Fe]$. As can be seen from Figure 2, the behaviour of J_{sc}, V_{oc} and FF is very different. While J_{sc} and FF start to decrease due to the iron–boron dissociation above iron concentrations of only $\sim 10^{10}$ cm^{-3}, V_{oc} shows the opposite behaviour and increases slightly in the range $[Fe] = 10^{10}$–10^{12} cm^{-3}. Only for iron concentrations above $\sim 10^{12}$ cm^{-3}, V_{oc} degrades as well. The increase in V_{oc} is only a weak effect for the industrial cell as surface recombination losses limit V_{oc}. In fact, for base resistivities below $\sim 3\,\Omega$ cm the increase in V_{oc} becomes practically undetectable in this type of solar cell. However, for a high-efficiency cell, the effect of increasing V_{oc} due to the Fe_iB_s dissociation is much more pronounced. Figure 3 shows the relative changes in J_{sc} and V_{oc} for the high-efficiency cell structure as a function of the iron concentration for three different doping concentrations. The lower the doping concentration of the silicon wafer, the more pronounced is the increase in V_{oc} due to the break-up of the iron–boron pairs. For the lowest doping level considered in this study, $N_{dop} = 10^{15}$ cm^{-3}, a maximum increase in V_{oc} of $\sim 5\%$ is observed at a relatively high iron contamination level of 2×10^{12} cm^{-3}. The strong increase in V_{oc} does, however, not lead to an increase in the cell efficiency as J_{sc} decreases at the same iron contamination level by 15%. As a generalised result, the dissociation of iron–boron pairs always leads to a degradation in J_{sc} and η, independent of the cell structure and the doping concentration.

The very different behaviour of V_{oc} and J_{sc} is due to the much larger injection level in the base of the cell under open-circuit than under short-circuit conditions. While under one-sun short-circuit conditions the excess carrier concentration within the base is always below the fixed crossover point characteristic of the iron–boron dissociation (see Figure 1), under open-circuit conditions it depends on the absolute value of the carrier lifetime whether the injection level is above or below the crossover point. Hence, at high iron levels corresponding to low lifetimes and low injection levels V_{oc} degrades, whereas at low iron contamination levels corresponding to higher lifetimes and higher injection levels V_{oc} increases.

The behaviour of the fill factor in Figure 2 might be surprising at first glance. After the dissociation of the iron–boron pairs, the fill factor shows a characteristic, very pronounced dependence on the iron contamination level. The fill factor drops sharply with increasing iron level, shows a minimum at iron levels between 10^{11} and 10^{12} cm^{-3} and increases again for higher iron concentrations. Such a behaviour has been reported before by

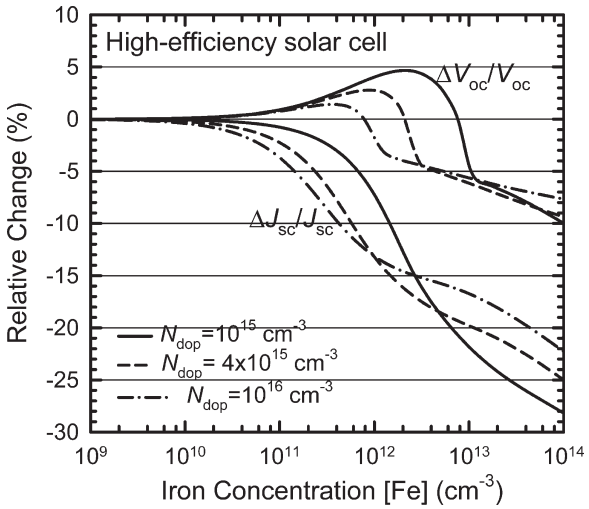

Figure 3. Relative changes in the open-circuit voltage V_{oc} and the short-circuit current density J_{sc} caused by a complete dissociation of Fe_iB_s pairs as a function of the iron concentration [Fe] for a high-efficiency solar cell at three different doping concentrations N_{dop}

Macdonald and Cuevas[10] and it has been consistently explained in terms of the strong injection level dependence of the carrier lifetime produced by the isolated Fe_i, resulting in a strongly increased ideality factor which peaks at a certain iron contamination level. A similar effect has been reported more recently for the boron–oxygen complex, which ultimately limits the efficiency in solar cells made on boron-doped oxygen-contaminated crystalline silicon.[11]

A useful quantity is the threshold iron contamination level $[Fe]_{th}$ above which a pronounced degradation in the different cell parameters due to the dissociation of the Fe_iB_s pairs can be observed. Figure 4 shows the calculated $[Fe]_{th}$ values above which a light-stimulated degradation of more than 1% in the corresponding cell parameter can be observed as a function of doping concentration N_{dop} for (a) the high-efficiency cell structure and (b) the industrial cell. Apart of the fill factor, which is a less important contributor to the total degradation, the curves corresponding to the V_{oc}, J_{sc} and η degradation are very similar for both cell structures for doping levels below $2 \times 10^{16}\,\mathrm{cm}^{-3}$. As can be seen from Figure 4, the V_{oc} degradation starts at iron contamination levels about two orders of magnitude higher than the threshold iron levels of the J_{sc} and η degradation. Hence,

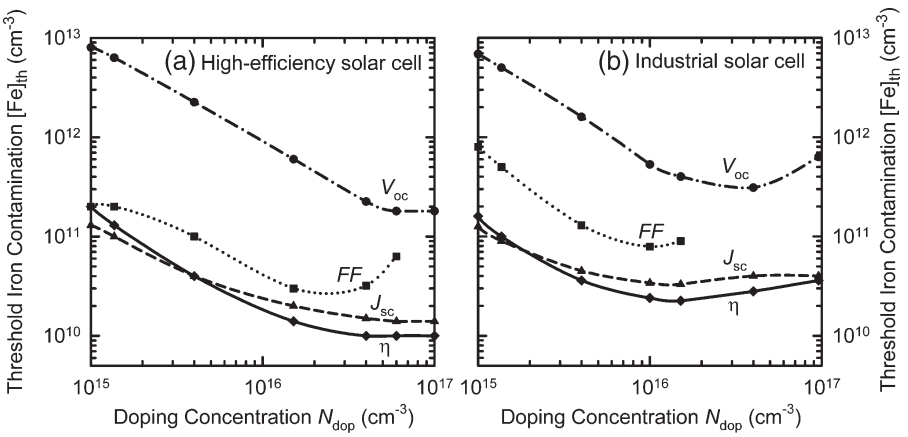

Figure 4. Threshold iron contaminations $[Fe]_{th}$ of the J_{sc}, V_{oc}, FF and η degradation caused by a complete dissociation of Fe_iB_s pairs as a function of doping concentration N_{dop} for (a) the high-efficiency cell structure; (b) the industrial cell

within a very broad range of iron concentrations only a degradation in J_{sc}, FF and η can be observed, whereas V_{oc} is constant, or even increases. This behaviour is specific to the iron–boron dissociation and may therefore be used for the identification of iron in silicon solar cells.

Fitting the data for $N_{dop} < 2 \times 10^{16}\,cm^{-3}$ in Figure 4 by a power law gives simple parameterisations for the threshold iron contamination levels ($[Fe]_{th}$ and N_{dop} in cm^{-3}):

$$[Fe]_{th,Voc} \simeq 7 \times 10^{27} \times N_{dop}^{-1} \tag{2}$$

$$[Fe]_{th,J_{sc}} \simeq [Fe]_{th,\eta} \simeq 2{\cdot}6 \times 10^{21} \times N_{dop}^{-0{\cdot}686} \tag{3}$$

Although these results are valid, independent of the cell structure, decreasing the cell thickness increases $[Fe]_{th}$ (reducing the cell thickness by a factor of two approximately doubles $[Fe]_{th}$).

The much higher threshold iron contamination levels of the V_{oc} degradation compared with that of the J_{sc}, FF and η degradation are solely due to the strong injection level dependence of the Fe_i-related carrier lifetime. Assuming a non-injection-dependent lifetime leads to $[Fe]_{th,Voc}$ values of the same order of magnitude or even below $[Fe]_{th,Jsc}$, $[Fe]_{th,FF}$ and $[Fe]_{th,\eta}$. In other words, if a crossover point were be absent the light-stimulated V_{oc} degradation would be of comparable magnitude or even more pronounced than the J_{sc} degradation.

Note that, from the results presented in this paper, the optimum value for the base doping concentration of a solar cell cannot directly be derived. However, it was recently shown by Geerligs and Macdonald[12] that the strong injection dependence of the Fe_i-related lifetime in silicon has in fact a crucial influence on the optimum base resistivity of a solar cell, shifting it to much higher values compared with the case of a constant lifetime.

All calculations in this study have been performed for a fixed illumination intensity of one sun. The use of different light intensities could give useful extra information. While light intensities above one sun should enhance the effect of increasing V_{oc} after Fe_iB_s dissociation and increase the iron threshold concentrations, intensities below one sun would result in the opposite trend. Hence, intensity-dependent measurements of the cell parameter changes under illumination could further facilitate the defect identification in silicon solar cells.

CONCLUSIONS

Dissociation of iron–boron pairs in crystalline silicon solar cells leads to a degradation in most cell parameters. In particular, short-circuit current and efficiency show a pronounced degradation, whereas the open-circuit voltage can increase by up to $\sim$5% for certain iron contamination levels. This phenomenon, which is particularly pronounced for high-efficiency cells, can be attributed to the strongly changing injection-dependent lifetime due to the iron–boron dissociation. The threshold iron contamination level of the open-circuit voltage degradation, marking the starting point of the degradation, is about one to two orders of magnitude higher than the threshold iron levels of the remaining cell parameters. Hence, up to relatively high iron concentrations only a degradation in short-circuit current, fill factor and efficiency may be observed, whereas the open-circuit voltage is constant or even increases, depending on the cell structure. This behaviour is characteristic of the iron–boron dissociation and may therefore in the future be interpreted as a sign of iron contamination problems in silicon solar cells.

Acknowledgements

The author is grateful to K. Bothe, J. Birkholz and D. Macdonald for helpful discussions and to R. Hezel for his continuous support. Funding was provided by the State of Lower Saxony and the German Federal Ministry for the Environment, Nature Conservation and Nuclear Safety (BMU) under contract number 0329846E. ISFH is a member of the German *Forschungsverbund Sonnenenergie*.

REFERENCES

1. Macdonald D, Cuevas A, Kinomura A, Nakano Y. Phosphorus gettering in multicrystalline silicon studied by neutron activation analysis. *Proceedings of the 29th IEEE Photovoltaic Specialists Conference*, New Orleans, LA, 2002; 285–288.
2. Istratov AA, Buonassisi T, MacDonald RJ, Smith AR, Schindler R, Rand JA, Kalejs J, Weber ER. Neutron activation analysis study of metal content of multicrystalline silicon for cost-efficient solar cells. *Proceedings of the 13th Workshop on Crystalline Silicon Solar Cell Materials and Processes*, Vail, CO, 2003; 158–161.
3. Ballif C, Peters S, Borchert D, Hässler C, Isenberg J, Schindler R, Warta W, Willeke G. Lifetime investigations of degradation effects in processed multicrystalline silicon wafers. *Proceedings of the 17th European Photovoltaic Solar Energy Conference*, Munich, Germany, 2001; 1818–1821.
4. Macdonald DH, Geerligs LJ, Azzizi A. Iron detection in crystalline silicon by carrier lifetime measurements for arbitrary injection and doping. *Journal of Applied Physics* 2004; **95**: 1021–1028.
5. Istratov AA, Hieslmair H, Weber ER. Iron and its complexes in silicon. *Applied Physics A* 1999; **69**: 13–44.
6. Kimerling LC, Benton JL. Electronically controlled reactions of interstitial iron in silicon. *Physica B* 1983; **116**: 297–300.
7. Macdonald D, Cuevas A, Wong-Leung J. Capture cross sections of the acceptor level of iron-boron pairs in *p*-type silicon by injection-level dependent lifetime measurements. *Journal of Applied Physics* 2001; **89**: 7932–7939.
8. Shockley W, Read WT. Statistics of the recombinations of holes and electrons. *Physical Review* 1952; **87**: 835–842.
9. Hall RN. Electron-hole recombination in germanium. *Physical Review* 1952; **87**: 387.
10. Macdonald D, Cuevas A. Reduced fill factors in multicrystalline silicon solar cells due to injection-level dependent bulk recombination lifetimes. *Progress in Photovoltaics: Research and Applications* 2000; **8**: 363–375.
11. Schmidt J, Cuevas A, Rein S, Glunz SW. Impact of light-induced recombination centres on the current-voltage characteristic of Czochralski silicon solar cells. *Progress in Photovoltaics: Research and Applications* 2001; **9**: 249–255.
12. Geerligs LJ, Macdonald D. Base doping and recombination activity of impurities in crystalline silicon solar cells. *Progress in Photovoltaics: Research and Applications* 2004; **12**: 309–316.